SAND2020-5750C

Inertia Estimation in Power Systems using Energy Storage and System Identification Techniques

Ujjwol Tamrakar, Nischal Guruwacharya, Niranjan Bhujel, Felipe Wilches-Bernal, Timothy M. Hansen, and Reinaldo Tonkoski

***Abstract*—Fast-frequency control strategies have been proposed in the literature to maintain inertial response of electric generation and help with the frequency regulation of the system. However, it is challenging to deploy such strategies when the inertia constant of the system is unknown and time-varying. In this paper, we present a data-driven system identification approach for an energy storage system (ESS) operator to identify the inertial response of the system (and consequently the inertia constant). The method is first tested and validated with a simulated genset model using small changes in the system load as the excitation signal and measuring the corresponding change in frequency. The validated method is then used to experimentally identify the inertia constant of a genset. The inertia constant of the simulated genset model was estimated with an error of less than 5% which provides a reasonable estimate for the ESS operator to properly tune the parameters of a fast-frequency controller.**

***Index Terms*—Energy storage systems, fast-frequency control, inertia, system identification, virtual inertia.**

I. Introduction

As the cost of renewable energy sources (RESs) competes with that of conventional generation, the future energy demand will be increasingly delivered by RES interfaced with power electronic converters. Converter-based generation does not typically contribute to the inertial response of a power system; as conventional rotational generator-based systems are displaced, the inertial response of the system is also displaced. The inertial response of power system also varies through time due to the influx of stochastic converter-based energy sources. This makes the power system susceptible to large frequency excursions, compromising frequency stability and overall system reliability as large frequency excursions may ultimately lead to system failure. Fast-frequency control strategies using energy storage systems (ESSs) have been proposed in the literature to emulate this lost inertia and maintain system frequency [1].

The inertial response of a power system is due to the release or absorption of the stored kinetic energy in large rotational generators during power imbalances. The inertia constant (H) is traditionally used to quantify this inertial response. A typical approach to estimate the overall inertia of a power system is based on the center of frequency method [2]. In this approach, the total inertia of a power system is estimated based only on the inertia constant of individual rotational generators. As these rotational generators are displaced by converter-based generation and ESSs, such an approach no longer represents the inertia constant of a power system given the different system dynamics. Exacerbating the problem, some converter-based generation are embedded with inertia emulation algorithms in the form of *virtual inertia* or fast-frequency support, contributing to the overall effective inertia of the system [3]. In addition, there are myriad loads that exhibit voltage and/or frequency dependency whose inertial response also needs to be considered. Thus there is a need to design effective inertial estimation techniques of a power system that does not rely on the conventional definition. Situational awareness regarding the effective inertia allows the system operator to design proper controllers to provide fast-frequency response and thus limit wide frequency variations. Similarly, it also allows system operators to procure and dispatch its resources effectively.

In [4], the inertia constant of a power system is estimated by solving the swing equation based on frequency transient measurements. A polynomial approximation with respect to time is applied to the transient frequency measurements to isolate the oscillations and noise in the measurement. The damping of the system has been neglected in this approach and, furthermore, these techniques are known to be susceptible to the identification of the exact time of frequency event onset and the order of the polynomial approximation [5]. System identification approaches using ambient frequency measurements have also been developed [6]. An online technique using phasor measurement unit (PMU) frequency measurements was proposed in [7]. The proposed method also uses the swing equation as the basis to determine the inertia constant, but instead relies on measurements of active power deviations and frequency from PMUs. The dependence of the method on frequency events however makes it unsuitable for tuning the parameters of the fast-frequency controller. In [8], an online identification of the inertial response of a system is performed

U. Tamrakar, N. Guruwacharya, N. Bhujel, T. M. Hansen, and R. Tonkoski are with the Electrical Engineering and Computer Science Department, South Dakota State University, Brookings, SD, USA. R. Tonkoski is the corresponding author: tonkoski@ieee.org.

F. Wilches-Bernal is with the Electric Power Systems Research, Sandia National Laboratories, Albuquerque, NM, USA.

This work is partially supported by the U.S. Department of Energy (DOE) Grant Number DE-SC0020281, the National Science Foundation (NSF) under Grant Number MRI-1726964, and the SDSU Joint Research, Scholarship and Creative Activity Challenge Fund.

The authors would like to thank Dr. Imre Gyuk, Director of Energy Storage Research, Office of Electricity Delivery and Energy Reliability for his funding and guidance on this research.

Sandia National Laboratories is a multi-mission laboratory managed and operated by National Technology and Engineering Solutions of Sandia, LLC., a wholly owned subsidiary of Honeywell International, Inc., for the U.S. Department of Energy National Nuclear Security Administration under contract DE-NA-0003525.

using a system identification approach on PMU recordings.

In this paper, we propose to use a data-driven system identification technique to estimate the inertial response, and thus the effective inertia constant, of the system. The power system under study is probed through small active power changes through an ESS that does not impact the operational stability of the system. Using the measured frequency and power measurements during the perturbations, a transfer function-based model is identified and the effective inertia constant is estimated. Results on a simulated genset model with a known inertia constant are first presented to validate the approach, followed by the estimation of effective inertia constant of a genset whose inertia constant is unknown. With the presented method, the ESS operator can estimate the unknown time-varying inertia of any generic power system and properly tune/control their device for fast-frequency strategies.

The paper is organized as follows: Section II introduces the modeled power system frequency dynamics. In Section III, the methodology used for the system identification process is described, followed by the simulation and the experimental setup. The results are presented and analyzed in Section IV, and the paper is concluded in Section V.

II. Modeling Frequency Dynamics

Power system frequency dynamics are usually modeled using the swing equation, which describes the behavior of generator frequency in response to an active power mismatch. We can represent the frequency dynamics of an entire power system through the dynamics of one *equivalent* generator [2]. Fig. 1 shows a linearized transfer function model that captures the frequency dynamics of the system.

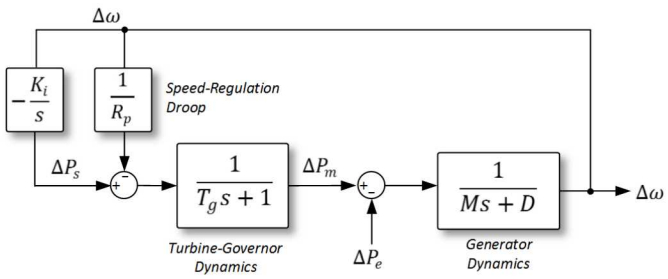

Fig. 1: Schematic representing the frequency dynamics of a power system.

The inertial response of the power system in response to an electrical load change of ΔP_e is governed by the equivalent inertia constant $M = 2H$ and damping constant D. This inertial response prevents the initial change in frequency until the the turbine-governor loop can control the frequency. The dynamics of the turbine-governor loop is typically represented by a first-order transfer function with time-constant T_g. This loop implements a speed-regulation droop to control the frequency by varying the mechanical power output ΔP_m. The secondary integral control loop with output power ΔP_s and the integral-gain K_i typically has very slow dynamics, and thus does not play a role in the inertial response of the system.

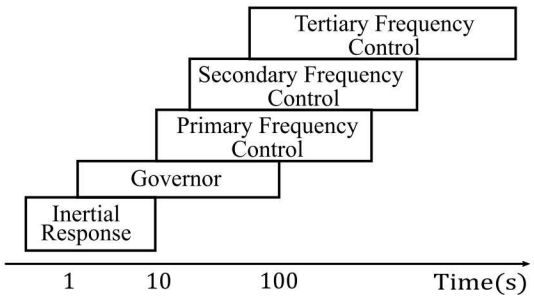

Fig. 2: Multiple time-scales of frequency dynamics in a typical power system.

The frequency dynamics of the power system can thus represented by the following set of differential equations:

$$M\Delta\dot{\omega} + D\Delta\omega = \Delta P_m - \Delta P_e \tag{1}$$

$$T_g\Delta\dot{P_m} + \Delta P_m = -R_p^{-1}\Delta\omega \tag{2}$$

In this paper, we are estimating the effective inertia constant $\hat{M}$ of the power system. The frequency dynamics of a power system has multiple time-scales, as depicted in Fig. 2. In the first few seconds after a frequency event, the frequency dynamics depends solely on the inertial response of the system. After the inertial response, the governor (or primary) controller then tries to limit the frequency drop and finally the secondary and/or tertiary controller acts to reduce the steady-state deviation in the frequency to zero. To estimate the inertia constant, we can decouple these time-scales. During the time-frame of interest, the secondary power ΔP_s and the mechanical power ΔP_m can be assumed to be zero, thus Eq. (1) can be reformulated as [6]:

$$M\dot{\Delta\omega} + D\Delta\omega = -\Delta P_e \tag{3}$$

The transfer function representing the frequency dynamics can be written as:

$$G(s) = \frac{\Delta\omega(s)}{\Delta P_e(s)} = -\frac{1}{Ms + D} \tag{4}$$

By identifying this transfer function, the inertia constant of the system can then be estimated.

III. System Identification Methodology

The basic concepts of system identification is first presented in this section. This is followed by a description of the methodology used to identify the inertia constants of a simulated and a real-genset using the system identification toolbox in MATLAB.

A. System Identification

A data-driven system identification approach can estimate the frequency dynamics of a power system. By probing the system to be identified with active power changes ΔP_e (in this work accomplished through an ESS), the corresponding response of the system frequency $\Delta\omega$ can be measured. Based on this input-output data, the unknown parameters of a transfer

function representing frequency dynamics can be identified. Fig. 3 illustrates the basic concepts of a system identification process. The input signal $u(t)$ and the output signal $y(t)$ are first measured from the unknown dynamic process to be identified. Because the logged data are discrete in nature (taken

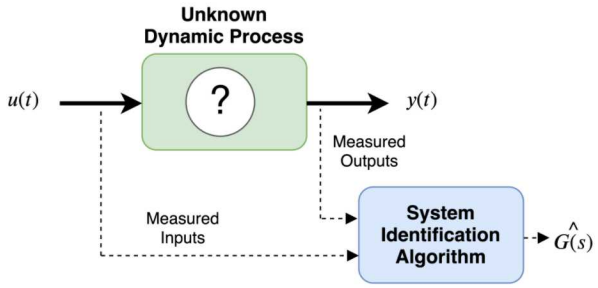

Fig. 3: Basic concept of system identification, which uses input and output measurements to identify an unknown dynamic process.

at a fixed sample rate), the relationship between the input and output can be defined as:

$$y(t) + a_1 y(t-1) + \cdots + a_n y(t-n) = b_1 u(t-1) + \cdots + b_m u(t-m) \quad (5)$$

where n and m represent the number of poles and zeros of the system, respectively, and a_n and b_m represent the parameters of the differential equation in Eq. (5) or the coefficients of the equivalent transfer function. In general, a dynamic system can then be represented as:

$$\hat{y}\,(t \mid \theta) = \phi^T \theta \quad (6)$$

In Eq. (6), θ represents the set of the unknown parameters/coefficients of the system, and $\phi(t)$ represents the set of inputs $u(t)$ and outputs $y(t)$ of the dynamic system defined as follows:

$$\theta = [a_1 \; a_2 \ldots a_n \; b_1 \; b_2 \ldots b_m]^T \quad (7)$$

$$\phi\,(t) = [-y(t-1) \cdots - y(t-n) \; u(t-1) \ldots u(t-m)]^T \quad (8)$$

Now, if we define Z^N as the set of known measurements and N is the overall input-output data points in the time interval $1 \leq t \leq N$:

$$Z^N = \{u(1), y(1), \ldots, u(N), y(N)\} \quad (9)$$

then the unknown parameters of the system, θ, are estimated by employing a least-squares method with the following cost-function [9]:

$$\min_{\theta} V_N = \frac{1}{N} \sum_{t=1}^{N} \|y(t) - \hat{y}(t \mid \theta)\|^2 \quad (10)$$

The fit of the model can be calculated using a metric, such as the normalized root-mean-square-error (NRMSE) defined as [10]:

$$NRMSE = 1 - \frac{\|y(t) - \hat{y}(t \mid \theta)\|}{\|y(t) - \text{mean}\,(\hat{y}(t|\theta))\|} \quad (11)$$

In a system identification procedure, the dataset must first be pre-processed to remove noise, offsets, and/or any unwanted trends in the data. Then a least-squares error approach described above is used to fit the model and identify the transfer function (training phase). Finally, to validate the identified transfer function (testing phase), the output from the identified model can be compared with the output determined experimentaly. Using different datasets for training and testing ensures the fitted models are applicable over a wide range of operation and prevents issues with overfitting [9].

B. Identification of Inertia Constant of a Simulated Genset Model

The system identification was initially conducted on a simulated genset model with a known inertia constant to test the validity of the proposed method. Fig. 4 shows the simulation setup used to perform system identification. A 3.125 MVA, 2.4 kV diesel-genset is used with a standard governor and AC1A-type excitation system as described in [11]. A fixed base load of 1 MW is always connected to the system. To excite the generator, various step changes in the active power were introduced through an ESS by setting different reference commands to the ESS for different perturbation power profiles and the resulting frequency changes were measured using a phase-locked-loop (PLL). Similarly, by measuring the generator terminal voltage v_{abc} and the output current i_{abc}, the change in electrical power was also computed and fed into the system identification routine mentioned in Section III-A.

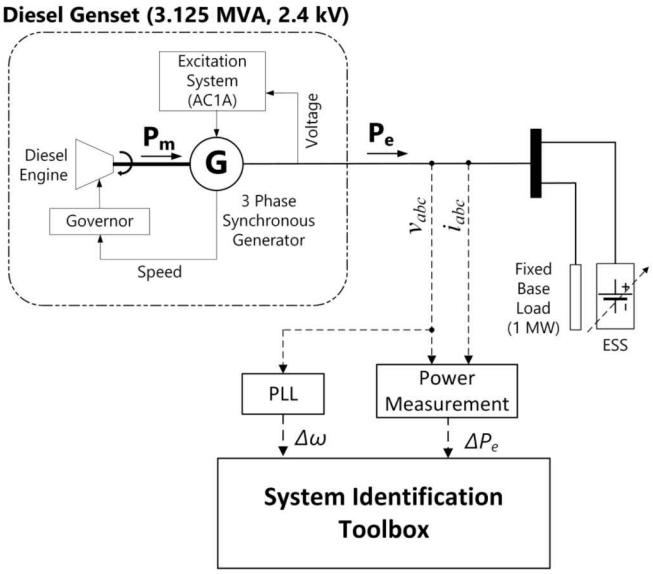

Fig. 4: Simulation setup used in MATLAB/Simulink for system identification. The system is excited through step changes in the active power introduced through an ESS. The corresponding frequency and active power measurements are fed into the system identification toolbox.

This routine is implemented by the system identification toolbox from MATLAB in this work. Three datasets were used

for training the model while a fourth dataset was collected for testing purposes as follows:

- Dataset S1: Step load changes of 31.25 kW (1% of generator size, used for training)
- Dataset S2: Step load changes of 62.50 kW (2% of generator size, used for training)
- Dataset S3: Step load changes of 312.50 kW (10% of generator size, used for training)
- Dataset S4: Step load changes of 781.25 kW (25% of generator size, used for testing)

Fig. 5 shows waveforms for Dataset S1 when the variable load was changed in steps of 31.25 kW. All the datasets were collected using a sample time of 0.1 ms. The input to the system is the active power change ΔP_e and the output is the change in frequency $\Delta\omega$ measured using a PLL. All the datasets were normalized with base values of 60 Hz and 3.125 MVA for the frequency and power, respectively. The input-output dataset are imported into the system identification toolbox. The system identification toolbox can be used to identify different types of models such as transfer functions, state-space models, ARX models, and other various non-linear models [10]. In this particular case, linear transfer function models are fit so the model is in the same form as in Fig. 1. After specifying the desired number of poles and zeros in the transfer function, the toolbox then identifies the coefficients of the transfer function through an iterative process that minimizes the prediction error using the cost function in Eq. (10). Transfer functions of increasing order were evaluated based on the fitness to both the testing and the training dataset using Eq. (11) and the model with the highest fit was chosen.

The identified higher-order models include the dynamics from inertial response and the primary and secondary frequency loops. Hence, to decouple these dynamics and to obtain the effective inertia value of the genset, the impulse response of the identified transfer function was computed as proposed in [6]. For example, the impulse response in time-domain of the first-order transfer function described in Eq. (4) is given by:

$$y(t) = -\frac{1}{M} exp\left(-\frac{D}{M}t\right) \tag{12}$$

Based on Eq. (12), at time $t = 0$, the impulse response leads to the reciprocal of the effective inertia of the system. A similar assumption can be made for the higher-order transfer function determined by the system identification process. By evaluating the unit-impulse response of the identified transfer function we can estimate the inertia constant of the genset.

C. Identification of Inertia Constant of a Genset Experimentally

After the methodology was validated with the simulation model, the same procedure was repeated for a 13 kW, 208 V natural gas genset (Kohler 15RES). In the experimental setup, the genset is loaded with a resistive load bank (Model L-63, Canon Load Banks) replicating the load perturbations from an ESS. Four datasets were collected based on the available

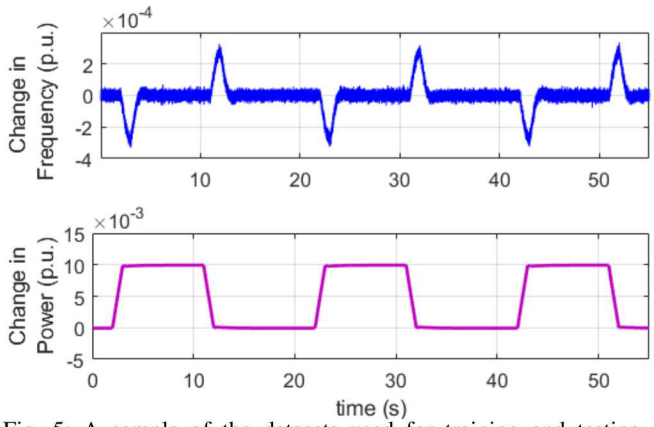

Fig. 5: A sample of the datasets used for training and testing of transfer function models. This particular figure shows the frequency of the system to 31.25 kW (0.01 p.u.) electrical load changes.

load changes in the resistive load bank. The frequency was again measured using a PLL and the power was computed through voltage and current measurements. The datasets are listed below:

- Dataset R1: Step load change from 1 to 6 kW (Training)
- Dataset R2: Step load change from 1 to 3 kW (Training)
- Dataset R3: Step load change from 0 to 5 kW (Training)
- Dataset R4: Random step load changes ranging from 1 to 8 kW (Testing)

The sample testing Dataset R1 is illustrated in Fig. 6. The sampling time was again set to 0.1 ms. The noise and the spikes in the power measurement were removed by using a moving average filter with a sliding window of 3000 samples. The moving average filter helps smooth out the measurements without introducing any significant delay.

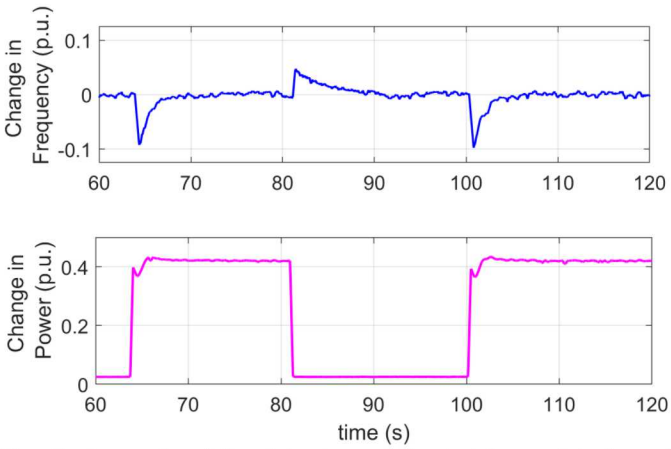

Fig. 6: A sample of the datasets used for training and testing of transfer function models for 13 kW genset. This particular figure shows the frequency of the genset to 5 kW active power changes.

IV. Results and Analysis

The results obtained from the identification of the inertia constant by simulation and experiment are presented and analyzed in this section.

A. Results from Simulated Genset Model

Table I summarizes the coefficients of the transfer functions identified using the different datasets. The fit for the identified second-order transfer functions with respect to the training and the testing dataset are also tabulated (calculated based on Eq. (11)). Initially, transfer functions of various orders were evaluated based on the fitness to both the training and the testing datasets. However, transfer functions higher than the second-order model did not provide any significant improvement in the fit and hence were not considered. In all three cases, approximately a 94% fit was achieved with both the training and the testing datasets. Increasing the amplitude of the excitation signal did not provide any improvement in the fits. The identified transfer functions obtained from different datasets are almost identical with only slight variations in the coefficients. This highlights the fact that the identified model is valid over a wide range of operation.

TABLE I: Transfer Functions Identified Using Simulated Genset

Dataset	Model Coefficients	Fitness to Training Data	Fitness to Test Data
S1	b_1 = -0.4954 b_0 = -0.0019 a_2 = 1.0000 a_1 = 6.7090 a_0 = 17.8900	94.52%	94.75%
S2	b_1 = -0.4931 b_0 = -0.0020 a_2 = 1.0000 a_1 = 6.6820 a_0 = 17.8200	94.73%	94.76%
S3	b_1 = -0.4863 b_0 = -0.0019 a_2 = 1.0000 a_1 = 6.5890 a_0 = 17.6100	94.91%	94.78%

Fig. 7 shows the unit-impulse response of all the three transfer functions that were identified. Based on the impulse response of the transfer function at time $t = 0$, the effective inertia of the system is calculated. The average of the inertia constant calculated from the unit-impulse response of the system at time $t = 0$ was taken. Thus, the estimated equivalent inertia constant $\hat{M}$ is computed to be 2.03. The actual equivalent inertia constant of the simulated genset model was 2.14. Thus, the inertia constant was estimated with a small error of approximately 5%. Even though we do not get an exact value, with this reasonable estimate the ESS operator can better the deploy fast-frequency control strategies in systems with unknown and/or time-varying inertia constants.

B. Results from Genset Experiments

Table II summarizes the coefficients of the second-order transfer functions identified using the different datasets collected from the 13 kVA genset available at SDSU's Microgrid Research Laboratory. The fitness of the model to the training and testing datasets, calculated using Eq. (11), are also provided. The fit is around 60%, which is considerably lower than for the simulated case with a second-order transfer function. The non-linearities in the response of an existing genset along

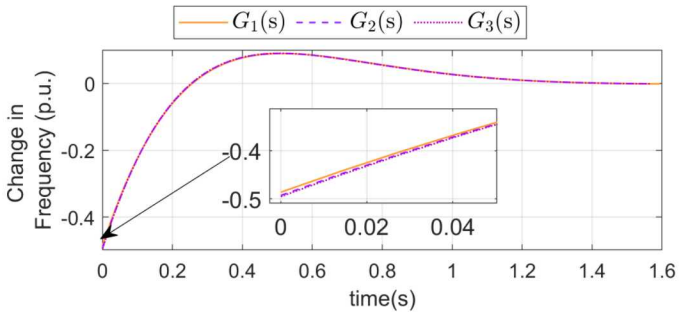

Fig. 7: Impulse response of the identified transfer functions from the simulated genset model. The inset highlights the impulse response at time $t = 0$.

TABLE II: Transfer Functions Identified Using Experimental Genset

Dataset	Model Coefficients	Fitness to Training Data	Fitness to Test Data
R1	b_1 = -0.99720 b_0 = -0.00006 a_2 = 1.00000 a_1 = 5.53262 a_0 = 3.24961	62.74%	55.55%
R2	b_1 = -1.94318 b_0 = -0.00081 a_2 = 1.00000 a_1 = 8.99629 a_0 = 5.03138	57.18%	57.43%
R3	b_1 = -0.98929 b_0 = 0.00121 a_2 = 1.0000 a_1 = 5.35941 a_0 = 2.89455	62.07%	57.78%

with the measurement noise are the most likely causes for the lower fit. Similar to the case with the simulated genset model, fitting higher-order models than a second-order model did not provide a significant improvement in the fit. Furthermore, a second-order model provides a sufficiently good fit around the timescale of interest (the inertial response of the genset). This can be visualized from Fig. 8, where it can be observed that even though there are errors in the overall fit, during the initial few seconds after the step load change, there is a relatively good agreement in the rate of frequency drop. Hence, we conclude the identified second-order models can be used to identify the inertia constant of the genset without significant errors.

Fig. 9 shows the unit-impulse response of the three identified transfer functions. Based on previous discussions, the reciprocal of the unit-impulse response of the identified transfer function at $t = 0$ gives the estimated effective inertia constant $\hat{M}$. For the genset, the estimated effective inertia constant $\hat{M}$ based on the unit-impulse response obtained from Datasets R1, R2 and R3 are 1.01, 0.51 and 1.00, respectively. The inertia constant estimated from Dataset R2 was higher compared to Datasets R1 and R3, indicating discrepancies in the inertia estimate. This may be due to the difference in the response of the genset for different step load changes and will require further testing.

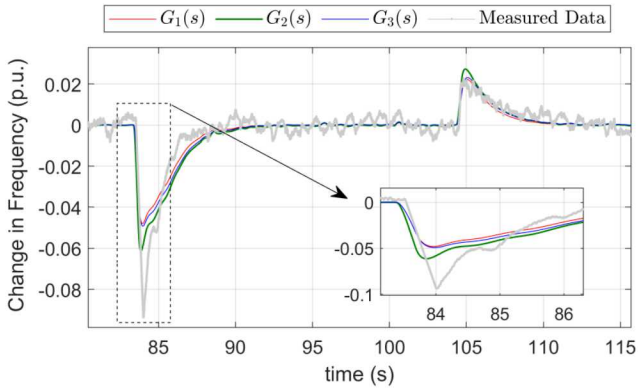

Fig. 8: Simulated and measured output of 13 kVA genset.

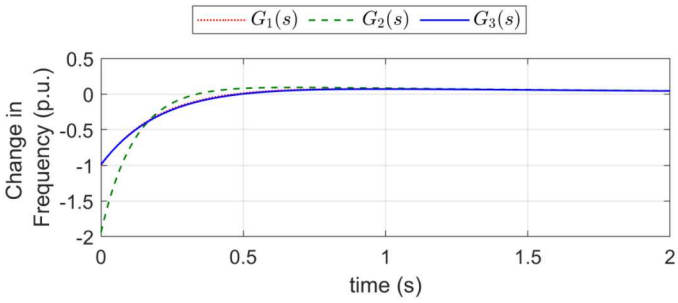

Fig. 9: Impulse response of the identified transfer functions of genset.

V. Conclusions

The inertia constant of a simulated and real-genset was identified using ESS and system identification techniques. With the simulated model, the system was excited through active power changes using an ESS. System identification technique was then utilized to identify the inertia constant with a relatively small error of less than 5% for the simulated model. The same methodology was then used to estimate the inertia constant of a genset. The generic method employed in this paper can easily be adopted by an ESS operator to identify the effective inertia constant of a power system where there are other elements such as inverters with fast-frequency control capabilities and/or frequency dependent loads that contribute to the overall inertia of a power system. The method currently requires the inertia constant to be estimated through offline system identification procedures. However, it can still provide the ESS operator with valuable insights to deploy and possibly coordinate fast-frequency control strategies so as to negate large frequency excursions to stochastic RESs.

References

[1] G. Delille, B. François, and G. Malarange, "Dynamic frequency control support: A virtual inertia provided by distributed energy storage to isolated power systems," in *IEEE PES Innovative Smart Grid Technologies Conference Europe (ISGT Europe)*, Oct. 2010, pp. 1–8.

[2] J. Schiffer, P. Aristidou, and R. Ortega, "Online estimation of power system inertia using dynamic regressor extension and mixing," *IEEE Transactions on Power Systems*, 2019.

[3] D. Groß, S. Bolognani, B. K. Poolla, and F. Dörfler, "Increasing the resilience of low-inertia power systems by virtual inertia and damping," in *Proceedings of IREP Symposium*, 2017, p. 64.

[4] T. Inoue, H. Taniguchi, Y. Ikeguchi, and K. Yoshida, "Estimation of power system inertia constant and capacity of spinning-reserve support generators using measured frequency transients," *IEEE Transactions on Power Systems*, vol. 12, no. 1, pp. 136–143, 1997.

[5] M. Shamirzaee, H. Ayoubzadeh, D. Farokhzad, F. Aminifar, and H. Haeri, "An improved method for estimation of inertia constant of power system based on polynomial approximation," in *IEEE Smart Grid Conference (SGC)*, 2014, pp. 1–7.

[6] K. Tuttelberg, J. Kilter, D. Wilson, and K. Uhlen, "Estimation of power system inertia from ambient wide area measurements," *IEEE Transactions on Power Systems*, vol. 33, no. 6, pp. 7249–7257, 2018.

[7] P. Wall and V. Terzija, "Simultaneous estimation of the time of disturbance and inertia in power systems," *IEEE Transactions on Power Delivery*, vol. 29, no. 4, pp. 2018–2031, 2014.

[8] J. Zhang and H. Xu, "Online identification of power system equivalent inertia constant," *IEEE Transactions on Industrial Electronics*, vol. 64, no. 10, pp. 8098–8107, 2017.

[9] L. Ljung, "System Identification: Theory for the User, 2nd ed." *Prentice Hall*, 1999.

[10] System identification toolbox. [Online]. Available: https://www.mathworks.com/products/sysid.html

[11] N. T. Janssen, R. A. Peterson, and R. W. Wies, "Development of a full-scale-lab-validated dynamic Simulink model for a stand-alone wind-powered microgrid," in *ASME Power Conference*, 2014.